

$1 \times N$ DWDM channel selective quantum frequency conversion

T. Arizono,¹ T. Kobayashi,^{1,2} S. Miki,³ H. Terai,³ T. Kodama,^{3,4} H. Shimoi,⁴ T. Yamamoto,^{1,2} and R. Ikuta^{1,2}

¹⁾Graduate School of Engineering Science, Osaka University, Osaka 560-8531, Japan

²⁾Center for Quantum Information and Quantum Biology, Osaka University, Osaka 560-8531, Japan

³⁾Advanced ICT Research Institute, National Institute of Information and Communications Technology, Hyogo, 651-2492, Japan

⁴⁾Hamamatsu Photonics K.K., Shizuoka, Japan

(*Electronic mail: ikuta.rikizo.es@osaka-u.ac.jp)

Dense Wavelength Division Multiplexing (DWDM) is a key technology for realizing high-capacity and flexible quantum communication networks. In addition, to realize the emerging quantum internet, quantum frequency conversion is also essential for bridging different quantum systems over optical fiber networks. In this work, we demonstrate a channel-selective quantum frequency conversion (CS-QFC), which allows active selection of the frequency of the converted photon from multiple DWDM channels. The 2.5 THz bandwidth of our CS-QFC system shows the ability to establish a 100-ch DWDM dynamic link from a single quantum system. It promises to increase the diversity of the quantum network.

I. INTRODUCTION

Frequency multiplexing in optical fiber networks is essential for high-speed and multi-user quantum communications. The generation and distribution of frequency-multiplexed entangled photon pairs based on broadband spontaneous parametric downconversion (SPDC), comparable to dense wavelength division multiplexing (DWDM) technologies, has been widely studied¹⁻⁹. However, SPDC-based photon sources will not always be applicable to the quantum internet^{10,11} which includes photonic systems and heterogeneous quantum matter systems such as atoms, ions, semiconductors, and superconductors. Experimental research to establish an entanglement between distant quantum matter systems via optical fiber-based quantum communication is increasingly active. In the studies, an efficient distribution of photons through optical fibers was achieved using quantum frequency conversion (QFC), which converts a wavelength of photons emitted from a quantum matter to a wavelength in the telecom band without destroying the entanglement¹²⁻²⁰. The process of QFC is based on nonlinear optical interaction with the use of a strong pump light at a frequency corresponding to the difference between the frequencies of the input and the converted photons. The QFC to a single telecom wavelength has been used in each experiment so far. However, in order to achieve any-to-any quantum communication between N parties assigned to N frequency channels in the DWDM network, based on the two-photon or single-photon interference at the midpoints, it is necessary to actively route each photon to the desired frequency channel so that the photons meet at the appropriate midpoints for the Bell measurement.

For this purpose, we demonstrate a QFC where the frequency of the converted photon can be actively selected from the DWDM channels. We call it channel selective QFC (CS-QFC) hereafter. The conceptual figure of the application of the CS-QFC to the multiparty quantum communication is shown in Fig. 1(a). The CS-QFC is achieved by selecting one of the multiple pump lasers, each frequency detuned from the others, for the nonlinear optical interaction. In the experiment, the CS-QFC is based on a second-order optical

nonlinearity in a periodically poled lithium niobate (PPLN) waveguide used for conventional QFC experiments. A single photon at 780 nm is input to the CS-QFC. Using one of seven pump lights around 1580 nm with a frequency detuning of 25 GHz, the signal photon is converted to wavelengths of around 1540 nm corresponding to the pump frequencies, and is distributed to different output channels of the DWDM demultiplexer (DeMux) without a serious channel crosstalk. The frequency range available for multiplexing demonstrated here is investigated to be over 2.5 THz. This shows the possibility of 100-mode frequency multiplexing for channel spacing of 25 GHz.

II. THEORY

The theory of the CS-QFC in this paper follows conventional QFCs based on difference frequency generation using a pump light at a single frequency mode, which we briefly review¹². The Hamiltonian of QFC from a signal mode at angular frequency ω_s to a converted mode at ω_c using a sufficiently strong pump light at $\omega_p = \omega_s - \omega_c$ is $H = i\hbar(\xi^* a_s a_c^\dagger - \xi a_s^\dagger a_c)$, where a_s and a_c are annihilation operators of the signal and converted modes. ξ is a coupling constant proportional to the complex amplitude of the pump light. By solving the Heisenberg equation, the time evolution of the converted mode with interaction time τ is obtained, which is regarded as the converted mode coming from the nonlinear optical medium. The annihilation operator of the mode denoted by b_c is described by $b_c = e^{-i\phi} \sin(\theta/2) a_s + \cos(\theta/2) a_c$, where ϕ is the phase of the pump light and $\theta/2 = |\xi| \tau$.

For the CS-QFC, we consider multiple pump lights at angular frequencies of $\omega_{p,i}$ for $1 \leq i \leq N$ including multiple communication round as shown in Figs. 1(a) and (b). When the pump light at $\omega_{p,i}$ is used in the T -th round of QFC, the annihilation operator $b_{c,T,i}$ of the converted mode at angular frequency $\omega_{c,i} = \omega_s - \omega_{p,i}$ from the nonlinear optical medium on T -th round is

$$b_{c,T,i} = e^{-i\phi_i} \sin(\theta_i/2) a_{s,T,i} + \cos(\theta_i/2) a_{c,T,i}, \quad (1)$$

where $[a_{s,T,i}, a_{s,T',j}^\dagger] = [a_{c,T,i}, a_{c,T',j}^\dagger] = \delta_{T,T'} \delta_{i,j}$, leading to $[b_{c,T,i}, b_{c,T',j}^\dagger] = \delta_{T,T'} \delta_{i,j}$. ϕ_i and θ_i depend on the complex amplitude of the pump light at $\omega_{p,i}$. From Eq. (1), the deterministic QFC of a photon from ω_s to $\omega_{c,i}$ is achieved for each round by satisfying $\theta_i = \pi$.

The above description of QFC holds for the region of frequencies satisfying the phase-matching condition $\Delta k = k(\omega_s) - k(\omega_{p,i}) - k(\omega_{c,i}) = 0$, where $k(\omega)$ is the wave number of photons at angular frequency ω . The larger value of $|\Delta k|$ leads to the lower value of the maximum conversion efficiency. In other words, the number N of the possible selections for the converted modes by the CS-QFC is limited by the phase-matching bandwidth. The phase-matching bandwidth related to the QFC is the same as that of SPDC photon pairs at $\omega_{p,i}$ and $\omega_{c,i}$ pumped by a laser light at ω_s . In typical experiments related to SPDC photon pairs at telecom wavelengths using PPLN waveguides, broad bandwidths larger than THz have been observed²¹.

For CS-QFC, only one pump light per round is used. If more than two pump lights are simultaneously input to the nonlinear optical medium, interactions between multiple signal modes and multiple converted modes with frequency spacings determined by the pump lights are induced. While such an interaction may be used for manipulating single-photon frequency combs, it will not be unsuitable for the deterministic frequency conversion of a photon at a single frequency mode to a different single frequency mode.

III. EXPERIMENTAL SETUP

The experimental setup for the CS-QFC is shown in Fig. 1(c). The CS-QFC has an input port for a signal light at 780 nm. The pump light for CS-QFC is prepared by a multi-channel wavelength tunable laser. The frequencies of the pump lasers can be independently set from 190.7 to 186.7 THz corresponding to the wavelengths from 1572.1 to 1605.7 nm. Each pump laser is connected to an optical shutter based on the InP/InGaAsP multiple quantum well (Thorlabs; BOA1004PXS) driven by a current source controller (Thorlabs; CLD1015) which has a switching speed of about 4 μ s. We can turn on and off the output power of each pump laser by modulating the voltage to the current source controller. The output power of the laser from the optical shutter can be adjusted by the operating current applied to the shutter. Each output light from the optical shutters is connected to a 16x1 frequency multiplexer (Mux) whose channel spacing is 25 GHz. The multiplexed light from the Mux is amplified by an erbium-doped fiber amplifier (EDFA) to a maximum power of 500 mW. The pump current of the EDFA is driven in the auto current control mode. With the proper setting of the current values applied to the optical shutters, the pump power after the amplification at each pump frequency is adjusted to a value giving a maximum conversion efficiency of CS-QFC.

The amplified pump light is combined with the signal light at 780 nm, and they are coupled to the PPLN-WG. The length of PPLN-WG is 40 mm. The DFG process in the PPLN-WG produces a frequency-converted light around 1540 nm.

The 1540 nm light coming from the PPLN-WG is separated from the signal light and the pump light by using a dichroic mirror (DM), a high-pass filter (HPF), respectively. Then, the converted light is coupled to a single-mode fiber (SMF) which is followed by a 1x16 frequency DeMux and a measurement apparatus such as an optical power meter, photo detectors (PDs), and superconducting nanostrip single photon detectors (SNSPDs) developed by Hamamatsu photonics and NICT.

In the demonstration of the CS-QFC, a 780 nm photon is prepared as the input signal photon by the SPDC process using another PPLN-WG (not shown). The pump light at 517 nm for SPDC generates 780 nm and 1540 nm photons. The 1540 nm photon heralds the 780 nm photon by the photon detection with a SNSPD after passing through a bandpass filter with a bandwidth of 10 GHz. The frequency-converted photon of the heralded 780 nm photon is detected by SNSPDs.

IV. EXPERIMENTAL RESULTS

A. Characterization of channel-selective frequency conversion

Before demonstrating the CS-QFC, we first investigated the conversion efficiencies of the device using continuous-wave laser light at 780 nm. To measure the pump power dependence of the conversion efficiency, we directly connected one of the tunable pump laser with the EDFA. In the experiment, we used pump light at frequencies of 190.7, 189.2, and 188.2 THz. The experimental results are shown in Fig. 2(a). The best fit of the experimental data to a function of $A \sin^2(\sqrt{BP})$ gives $(A, B) = (0.38, 0.010 \text{ mW}^{-1})$, $(0.39, 0.013 \text{ mW}^{-1})$ and $(0.37, 0.012 \text{ mW}^{-1})$ for the pump frequencies of 190.7, 189.2 and 188.2 THz, respectively. From the results, the pump power dependencies of the conversion efficiencies are similar across various pump frequencies. While the values of B are not exactly equal, the passive adjustment of appropriate electric currents applied to the shutters of the pump channels followed by the EDFA at a constant gain can achieve the frequency conversion process with the maximum conversion efficiencies of η_{max} in each channel as we explained. By a similar logic, the conversion efficiency can be equalized across all channels. Consequently, we conclude that the frequency conversion system is applicable to the large-scale frequency multiplexing.

Next, we measured the dependence of the maximum conversion efficiencies on the frequencies of the pump light. We increased the pump frequencies in 0.5 THz steps over a configurable range. In this experiment, the temperature of the PPLN-WG is optimized for the conversion using the pump light at 189.2 THz. The maximum conversion efficiency for each setting of the pump frequency was measured by fine-tuning the pump power in the vicinity of 200 mW from the result in Fig. 2(a). The experimental result of the dependence of the maximum conversion efficiencies is shown in Fig. 2(b). We can see that in the range of the pump frequency 188.2 – 190.7 THz (shaded area), which corresponds to the

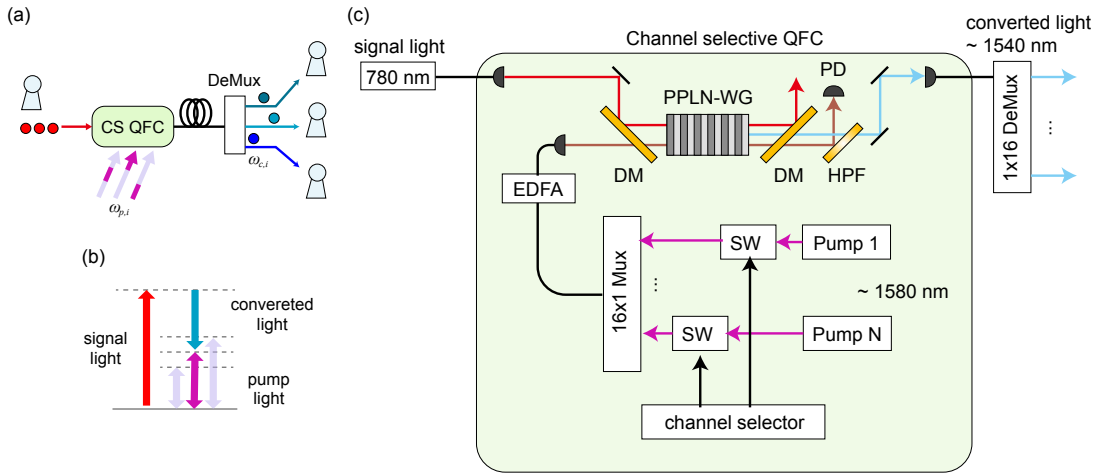


FIG. 1. (a) Concept of CS-QFC. (b) Energy diagram of CS-QFC. (c) Experimental setup.

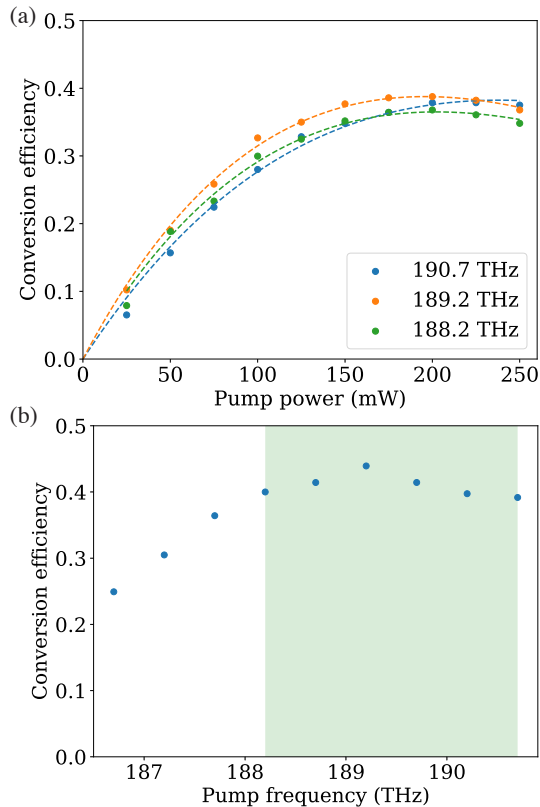


FIG. 2. (a) Conversion efficiencies for pump lights at the frequencies of 190.7, 190.2, and 189.7 THz. (b) The dependency of the maximum conversion efficiencies on the frequencies of the pump light.

pump wavelength range 1592.9 – 1572.1 nm, maximum conversion efficiencies of about 40% or even higher are obtained. If we consider the above range of 2.5 THz range as the acceptable range to be used as selectable channels for CS-QFC, the number of channels for DWDM is 100 with a channel spacing of 25 GHz. The wideband acceptable region of CS-QFC is

comparable to the region of the signal and idler photon pairs generated by the SPDC process, which has been demonstrated in Ref.²¹.

We characterized the switching property of the frequency conversion. We used two pump lasers at the frequencies of 189.731 and 189.756 THz with the detuning of 25 GHz, which convert the signal light into the output frequency channel of 194.5 and 194.475 THz, respectively. The corresponding converted wavelengths are 1541.35 and 1541.55 nm. In the experiment, we switched the two pump lights every 100 μ s, 3 μ s or 1 μ s and measured the converted light separated by the DeMux followed by the PDs and the digital sampling oscilloscope. The experimental result is shown in Fig. 3. As a reference, we monitored the pump power reflected by the HPF, as represented by the green curves in Fig. 3. For the case of the switching interval of 100 μ s, frequency-converted lights at the two channels are switched much faster than the switching interval. In contrast, for the cases of switching interval of 3 μ s and 1 μ s, we see the switching speed is comparable with the interval time. By determining the rise/fall time by the time it takes for the pulse to go from/to 10 to/from 90%, the estimated rise and fall times are 0.5 μ s. Consequently, a switching interval slower than 0.5 μ s is required for the ideal operation of this device. It is important to note that the observed pump power shows a transient response when the pump light is turned on and off. We guess the reason might be that the light power stored in the EDFA is released at once. Despite the behavior of the pump light during switching, the converted light is insensitive to the transient response of the pump light. This is because the conversion efficiency determined by $A \sin(\sqrt{BP})$ is insensitive to changes in pump power around the maximum conversion efficiency.

B. CS-QFC using a single photon input

We performed the demonstration of CS-QFC using 7-ch pump lights at frequencies from 189.383 to 189.533 THz with

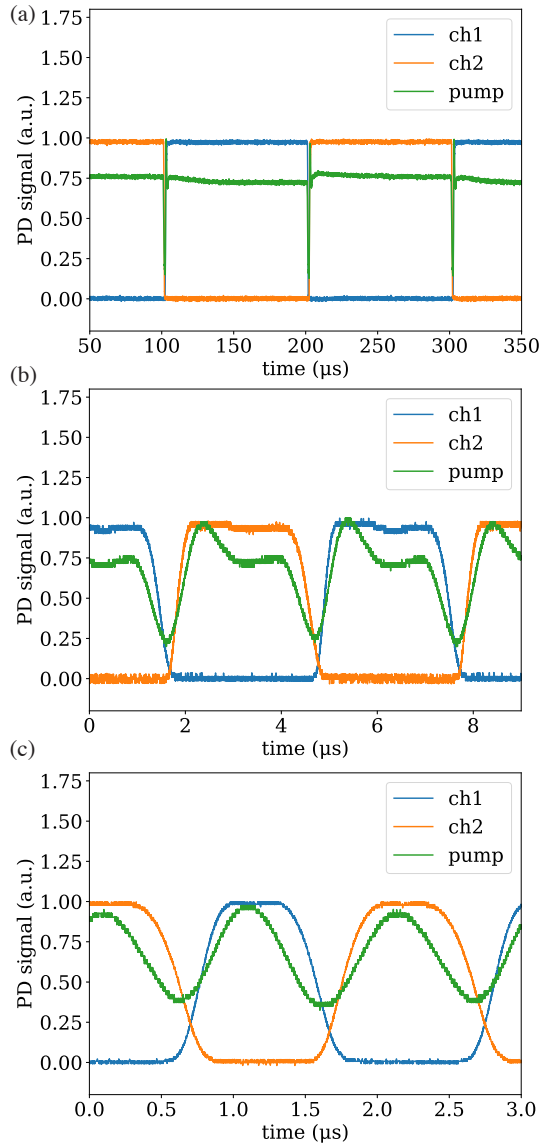


FIG. 3. Observed signals of the converted light (blue: 194.5 THz, orange: 194.475 THz) and the pump light (green) observed during switching between the two pump lights at rates of (a) 100 μ s, (b) 3 μ s, and (c) 1 μ s.

the step of 25 GHz. The prepared SPDC photon pairs at 780 and 1541 nm before QFC have the cross-correlation function of 18.22 ± 0.04 . The 780 nm heralded single photon is converted to the frequencies from 194.85 to 194.7 THz, that are from channel 1 to channel 7 of the DeMux. To reduce the Raman scattering noises, we added the two bandpass filters with the bandwidths of 12 nm and 1.7 nm before the 1x16 DeMux. The experimental results of the observed cross-correlation functions between the heralding and converted photons are shown in Fig. 4(a). The accumulation time was 180 sec and the width of the time bin was 34 ps. By using these histograms of Fig. 4(a) and the time window of 476 ps, the estimated cross-correlations in each frequency channel for all pump frequencies are summarized in Fig. 4(b). As expected, a high

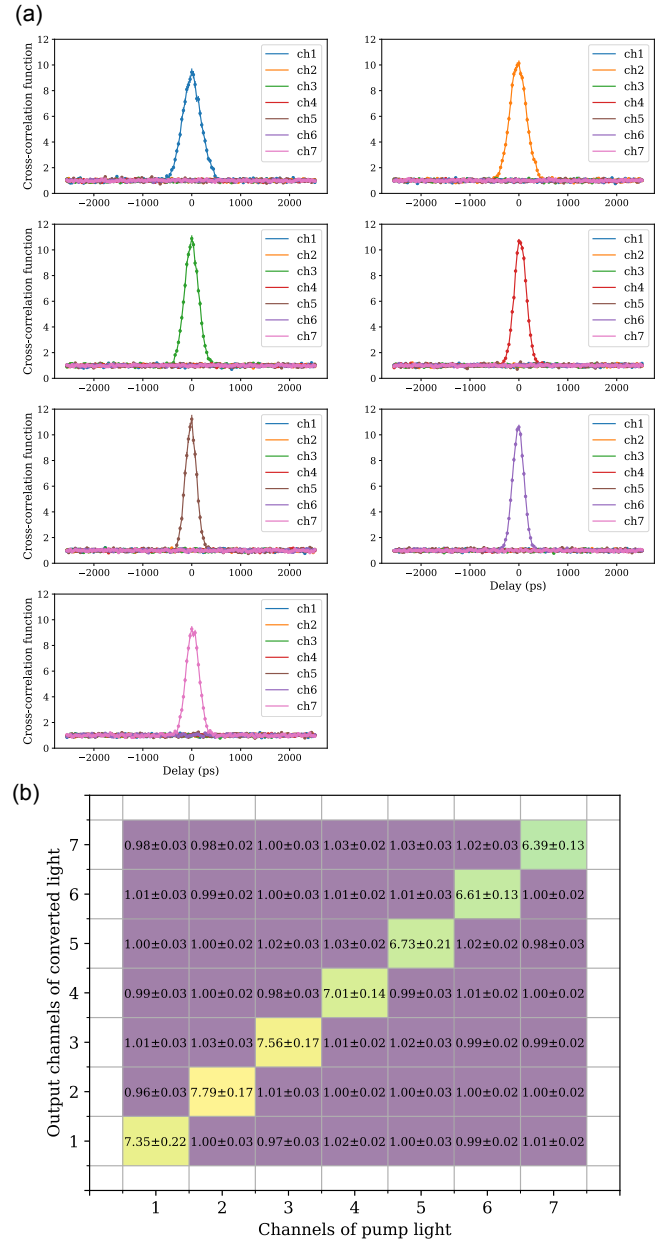


FIG. 4. (a) The observed coincidence histograms of the time difference between the heralding photon and the converted photons. The coincidence counts are normalized as cross-correlation functions. (b) The estimated cross-correlation with the time window of 476 ps in every output frequency channel for all pump frequencies.

cross-correlation function was observed in the output channel corresponding to the pump frequency due to the existence of the photons converted by the signal photons correlated with the heralding photon. This shows that the converted photons were observed only in the desired output channels without serious crosstalk on the other channels. We thus conclude the CS-QFC was successfully demonstrated.

V. DISCUSSION

In the experiment, we showed that the bandwidth of the CS-QFC is ~ 2.5 THz, which corresponds to 100 switchable channels with a channel spacing of 25 GHz. The bandwidth is determined by the acceptance bandwidth of the PPLN-WG. A shorter PPLN waveguide allows a larger number of switchable frequency channels, at the expense of a higher pump power required for the maximum conversion efficiency. While we have demonstrated the CS-QFC with only 7 output channels between 175 GHz, at least 100-ch pump lasers, including the fast switches, are needed to effectively utilize the 2.5 THz bandwidth. One way to achieve this with a low cost of the laser source preparation is to use of the wavelength-tunable laser as a pump light. According to the state of the art of ultrafast tunable laser²², electro-optic laser frequency tuning is possible at a rate of 12 PHz/s while maintaining the narrow linewidth of \sim kHz. Using this laser, we can take $2 \mu\text{s}$ to tune the 25 GHz frequency. For faster switching, multiple tunable lasers combined with a fast N -to-1 optical switch can be used. A commercially available N -to-1 switch²³ has a switching speed of 10 ns. It is sufficient to improve the switching speed of the ultrafast tunable laser described above. Another way to reduce the cost of the light source is the use of an optical frequency comb split by DeMux with a spacing of 25 GHz instead of 100-ch pump lasers.

As discussed above, there are several candidates for the pump light of CS-QFC. To apply the CS-QFC to quantum communication including quantum matter systems, not only the switching speed of the pump light but also the other properties such as the linewidth and stability are important to achieve high rate and high fidelity quantum communication. For the communication rate, the channel switching speed τ_s must be much faster than the temporal width τ_c of the photons is required in order not to decrease the rate. For the fidelity, because the indistinguishability of photons arrived from different nodes is crucial, the pump light with the frequency fluctuations degrades the visibility of the interference. Therefore, sufficient stability of the pump frequency is required. For example, a 780 nm photon entangled with a Rb atom is generated using D2 line transition with a linewidth of 6 MHz and a temporal width of $\tau_c = 26 \text{ ns}$ ^{24,25}. In this case, the CS-QFC with a switching speed of $\tau_s \sim 10 \text{ ns}$ will not significantly affect the communication rate. For the fidelity, a sufficiently narrow linewidth and frequency stability much less than 6 MHz is required for the pump light to keep the initial linewidth of the photon. This suggests multiple stable lasers or a frequency comb may be more promising than a conventional tunable laser for the pump light. The above discussion is just an example of the quantum communication using Rb atoms. In practice, it is crucial to use a suitable pump light that meets the required switching speed and stability, tailored to the specific parameters of other quantum systems, multiplexing methods, and quantum communication protocols to be implemented.

VI. CONCLUSION

We have demonstrated the CS-QFC, which converts a frequency of a signal photon to another frequency actively switchable at each round of the conversion process. The switchable bandwidth of the CS-QFC is 2.5 THz, achieving 100 frequency channels with a channel spacing of 25 GHz. Using a heralded single photon generated by the SPDC, we successfully demonstrated the CS-QFC with the 7 output channels switchable by using one of the seven different frequencies of the pump light. Namely, the converted photons were observed in the desired output channel expected from the pump frequency, while preserving the non-classical photon statistics without the crosstalk to the other different channels. We have discussed the possibility of applying the CS-QFC to the conversion of photons emitted from the Rb atom by considering the candidates for the configuration of the pump light preparation using commercially available devices and state-of-the-art technologies.

The demonstrated CS-QFC provides switching functionality to the quantum interface, which selectively converts to the wavelengths in the WDM channels from a single frequency around the visible range of photons emitted from quantum matter systems. Combining CS-QFC and frequency converters on WDM channels²⁶⁻³⁰ allows for more flexible routing of the photons. This capability is valuable for realizing entanglement distribution with switching network designs^{31,32} and a DWDM-compatible quantum internet.

ACKNOWLEDGMENTS

This work was supported by Moonshot R & D, JST JPMJMS2066, JST JPMJMS226C; R & D of ICT Priority Technology Project JPMI00316; FOREST Program, JST JPMJFR222V. T.Y. and R.I. acknowledge the members of the Quantum Internet Task Force for the comprehensive and interdisciplinary discussions on the quantum internet.

¹H. C. Lim, A. Yoshizawa, H. Tsuchida, and K. Kikuchi, "Distribution of polarization-entangled photon-pairs produced via spontaneous parametric down-conversion within a local-area fiber network: Theoretical model and experiment," *Opt. Express* **15**, 7853–7862 (2007).

²H. C. Lim, A. Yoshizawa, H. Tsuchida, and K. Kikuchi, "Broadband source of telecom-band polarization-entangled photon-pairs for wavelength-multiplexed entanglement distribution," *Opt. Express* **16**, 16052–16057 (2008).

³H. C. Lim, A. Yoshizawa, H. Tsuchida, and K. Kikuchi, "Wavelength-multiplexed distribution of highly entangled photon-pairs over optical fiber," *Opt. Express* **16**, 22099–22104 (2008).

⁴Z.-Y. Zhou, Y.-K. Jiang, D.-S. Ding, B.-S. Shi, and G.-C. Guo, "Actively switchable nondegenerate polarization-entangled photon-pair distribution in dense wave-division multiplexing," *Phys. Rev. A* **87**, 045806 (2013).

⁵J. Ghalbouni, I. Agha, R. Frey, E. Diamanti, and I. Zaquine, "Experimental wavelength-division-multiplexed photon-pair distribution," *Opt. Lett.* **38**, 34–36 (2013).

⁶D. Aktas, B. Fedrici, F. Kaiser, T. Lunghi, L. Labonté, and S. Tanzilli, "Entanglement distribution over 150 km in wavelength division multiplexed channels for quantum cryptography," *Laser Photon. Rev.* **10**, 451–457 (2016).

- ⁷S. Wengerowsky, S. K. Joshi, F. Steinlechner, H. Hübel, and R. Ursin, “An entanglement-based wavelength-multiplexed quantum communication network,” *Nature* **564**, 225–228 (2018).
- ⁸S. K. Joshi, D. Aktas, S. Wengerowsky, M. Lončarić, S. P. Neumann, B. Liu, T. Scheidl, G. C. Lorenzo, Ž. Samec, L. Kling, A. Qiu, M. Razavi, M. Stipčević, J. G. Rarity, and R. Ursin, “A trusted node-free eight-user metropolitan quantum communication network,” *Sci. Adv.* **6**, aba0959(2020).
- ⁹A. Mueller, S. I. Davis, B. Korzh, R. Valivarthi, A. D. Beyer, R. Youssef, N. Sinclair, C. Peña, M. D. Shaw, and M. Spiropulu, “High-rate multiplexed entanglement source based on time-bin qubits for advanced quantum networks,” *Optica Quantum* **2**, 64 (2024).
- ¹⁰H. J. Kimble, “The quantum internet,” *Nature* **453**, 1023–1030 (2008).
- ¹¹S. Wehner, D. Elkouss, and R. Hanson, “Quantum internet: A vision for the road ahead,” *Science* **362**, eaam9288 (2018).
- ¹²R. Ikuta, Y. Kusaka, T. Kitano, H. Kato, T. Yamamoto, M. Koashi, and N. Imoto, “Wide-band quantum interface for visible-to-telecommunication wavelength conversion,” *Nature Communications* **2**, 537 (2011).
- ¹³R. Ikuta, T. Kobayashi, T. Kawakami, S. Miki, M. Yabuno, T. Yamashita, H. Terai, M. Koashi, T. Mukai, T. Yamamoto, and N. Imoto, “Polarization insensitive frequency conversion for an atom-photon entanglement distribution via a telecom network,” *Nature Communications* **9**, 1997 (2018).
- ¹⁴M. Bock, P. Eich, S. Kucera, M. Kreis, A. Lenhard, C. Becher, and J. Eschner, “High-fidelity entanglement between a trapped ion and a telecom photon via quantum frequency conversion,” *Nature Communications* **9**, 1998 (2018).
- ¹⁵A. Tchebotareva, S. L. Hermans, P. C. Humphreys, D. Voigt, P. J. Harmsma, L. K. Cheng, A. L. Verlaan, N. Dijkhuizen, W. de Jong, A. Dréau, and R. Hanson, “Entanglement between a diamond spin qubit and a photonic time-bin qubit at telecom wavelength,” *Physical Review Letters* **123**, 063601 (2019).
- ¹⁶V. Krutyanskiy, M. Canteri, M. Meraner, J. Bate, V. Krčmaršky, J. Schupp, N. Sangouard, and B. Lanyon, “Telecom-wavelength quantum repeater node based on a trapped-ion processor,” *Physical Review Letters* **130**, 213601 (2023).
- ¹⁷E. Bersin, M. Sutula, Y. Q. Huan, A. Suleymanzade, D. R. Assumpcao, Y.-C. Wei, P.-J. Stas, C. M. Knaut, E. N. Knall, C. Langrock, N. Sinclair, R. Murphy, R. Riedinger, M. Yeh, C. Xin, S. Bandyopadhyay, D. D. Sukachev, B. Machielse, D. S. Levonian, M. K. Bhaskar, S. Hamilton, H. Park, M. Lončar, M. M. Fejer, P. B. Dixon, D. R. Englund, and M. D. Lukin, “Telecom networking with a diamond quantum memory,” *PRX Quantum* **5**, 010303 (2024).
- ¹⁸Y. Zhou, P. Malik, F. Fertig, M. Bock, T. Bauer, T. van Leent, W. Zhang, C. Becher, and H. Weinfurter, “Long-lived quantum memory enabling atom-photon entanglement over 101 km of telecom fiber,” *PRX Quantum* **5**, 020307 (2024).
- ¹⁹J.-L. Liu, X.-Y. Luo, Y. Yu, C.-Y. Wang, B. Wang, Y. Hu, J. Li, M.-Y. Zheng, B. Yao, Z. Yan, D. Teng, J.-W. Jiang, X.-B. Liu, X.-P. Xie, J. Zhang, Q.-H. Mao, X. Jiang, Q. Zhang, X.-H. Bao, and J.-W. Pan, “Creation of memory–memory entanglement in a metropolitan quantum network,” *Nature* **629**, 579–585 (2024).
- ²⁰C. M. Knaut, A. Suleymanzade, Y.-C. Wei, D. R. Assumpcao, P.-J. Stas, Y. Q. Huan, B. Machielse, E. N. Knall, M. Sutula, G. Baranes, N. Sinclair, C. De-Eknankul, D. S. Levonian, M. K. Bhaskar, H. Park, M. Lončar, and M. D. Lukin, “Entanglement of nanophotonic quantum memory nodes in a telecom network,” *Nature* **629**, 573–578 (2024).
- ²¹Z. Zhang, C. Yuan, S. Shen, H. Yu, R. Zhang, H. Wang, H. Li, Y. Wang, G. Deng, Z. Wang, L. You, Z. Wang, H. Song, G. Guo, and Q. Zhou, “High-performance quantum entanglement generation via cascaded second-order nonlinear processes,” *npj Quantum Information* **7**, 123 (2021).
- ²²V. Snigirev, A. Riedhauser, G. Lihachev, M. Churaev, J. Riemensberger, R. N. Wang, A. Siddharth, G. Huang, C. Möhl, Y. Popoff, U. Drechsler, D. Caimi, S. Hönl, J. Liu, P. Seidler, and T. J. Kippenberg, “Ultrafast tunable lasers using lithium niobate integrated photonics,” *Nature* **615**, 411–417 (2023).
- ²³K. Nashimoto, N. Tanaka, M. LaBuda, D. Ritums, J. Dawley, M. Raj, D. Kudzuma, and T. Vo, “High-speed plzt optical switches for burst and packet switching,” *2nd International Conference on Broadband Networks*, 2005. **2**, 1118–1123 (2005).
- ²⁴D. A. Steck, “Rubidium 87 d line data,” (2001), <http://steck.us/alkalidata>.
- ²⁵J. Hofmann, M. Krug, N. Ortegel, L. Gérard, M. Weber, W. Rosenfeld, and H. Weinfurter, “Heralded entanglement between widely separated atoms,” *Science* **337**, 72–75 (2012).
- ²⁶C. Joshi, A. Farsi, S. Clemmen, S. Ramelow, and A. L. Gaeta, “Frequency multiplexing for quasi-deterministic heralded single-photon sources,” *Nature Communications* **9**, 847 (2018).
- ²⁷Y. L. Lee, C. Jung, Y.-C. Noh, M. Y. Park, C. C. Byeon, D.-K. Ko, and J. Lee, “Channel-selective wavelength conversion and tuning in periodically poled ti:linbo3 waveguides,” *Optics Express* **12**, 2649 (2004).
- ²⁸P. Fisher, R. Cernansky, B. Haylock, and M. Lobino, “Single photon frequency conversion for frequency multiplexed quantum networks in the telecom band,” *Physical Review Letters* **127**, 023602 (2021).
- ²⁹P.-C. Wang, O. Pietx-Casas, M. Falamarzi Askarani, and G. C. do Amaral, “Proposal and proof-of-principle demonstration of fast-switching broadband frequency shifting for a frequency-multiplexed quantum repeater,” *Journal of the Optical Society of America B* **38**, 1140 (2021).
- ³⁰R. Ikuta, M. Yokota, T. Kobayashi, N. Imoto, and T. Yamamoto, “Optical frequency tweezers,” *Phys. Rev. Appl.* **17**, 034012 (2022).
- ³¹R. J. Drost, T. J. Moore, and M. Brodsky, “Switching networks for pairwise-entanglement distribution,” *Journal of Optical Communications and Networking* **8**, 331–342 (2016).
- ³²M. Koyama, C. Yun, A. Taherkhani, N. Benchasattabuse, B. O. Sane, M. Hajdušek, S. Nagayama, and R. Van Meter, “Optimal switching networks for paired-egress bell state analyzer pools,” *arXiv preprint arXiv:2405.09860* (2024).